# Chapter 7
# Hydration and Nanoconfined Water: Insights from Computer Simulations

**Laureano M. Alarcón, J.A. Rodríguez Fris, Marcela A. Morini, M. Belén Sierra, S.A. Accordino, J.M. Montes de Oca, Viviana I. Pedroni, and Gustavo A. Appignanesi**

**Abstract** The comprehension of the structure and behavior of water at interfaces and under nanoconfinement represents an issue of major concern in several central research areas like hydration, reaction dynamics and biology. From one side, water is known to play a dominant role in the structuring, the dynamics and the functionality of biological molecules, governing main processes like protein folding, protein binding and biological function. In turn, the same principles that rule biological organization at the molecular level are also operative for materials science processes that take place within a water environment, being responsible for the self-assembly of molecular structures to create synthetic supramolecular nanometrically-sized materials. Thus, the understanding of the principles of water hydration, including the development of a theory of hydrophobicity at the nanoscale, is imperative both from a fundamental and an applied standpoint. In this work we present some molecular dynamics studies of the structure and dynamics of water at different interfaces or confinement conditions, ranging from simple model hydrophobic interfaces with different geometrical constraints (in order to single out curvature effects), to self-assembled monolayers, proteins and phospholipid membranes. The tendency of the water molecules to sacrifice the lowest hydrogen bond (HB) coordination as possible at extended interfaces is revealed. This fact makes the first hydration layers to be highly oriented, in some situations even resembling the structure of hexagonal ice. A similar trend to maximize the number of HBs is shown to hold in cavity filling, with small subnanometric hydrophobic cavities remaining empty while larger cavities display an alternation of filled and dry states with a significant inner HB network. We also study interfaces with complex chemical and geometrical nature in order to determine how different conditions affect the local hydration properties. Thus, we show some results for protein hydration and, particularly, some preliminary

L.M. Alarcón • J.A. Rodríguez Fris • M.A. Morini • M.B. Sierra • S.A. Accordino • J.M. Montes de Oca • V.I. Pedroni • G.A. Appignanesi (✉)
Departamento de Química and INQUISUR-UNS-CONICET, Universidad Nacional del Sur, Av. Alem 1253, 8000 Bahía Blanca, Argentina
e-mail: lalarcon@uns.edu.ar; mamorini@criba.edu.ar; mbsierra@uns.edu.ar; pedroni@criba.edu.ar; appignan@criba.edu.ar



E.A. Disalvo (ed.), *Membrane Hydration*, Subcellular Biochemistry 71,
DOI 10.1007/978-3-319-19060-0_7

studies on membrane hydration. Finally, calculations of a local hydrophobicity measure of relevance for binding and self-assembly are also presented. We then conclude with a few words of further emphasis on the relevance of this kind of knowledge to biology and to the design of new materials by highlighting the context-dependent and non-additive nature of different non-covalent interactions in an aqueous nanoenvironment, an issue that is usually greatly overlooked.

**Keywords** Hydration water • Confined water • Geometry • Computer simulation • H-bonds • Self assembled monolayers • Hydrophobicity • Density fluctuations

## 7.1 Introduction

The behavior of water at interfaces and under nanoconfinement is quite different from that at bulk conditions, as many experimental and theoretical studies have demonstrated (Huang and Chandler 2000; Huang et al. 2003; Bizzarri and Cannistraro 2002; Vitkup et al. 2000; Choudhury and Montgomery Pettitt 2005; Stanley et al. 2007; Giovambattista et al. 2008; Rasaiah et al. 2008; Berne et al. 2009; Malaspina et al. 2010; Alarcón et al. 2011; Gelman Constantin et al. 2011; Accordino et al. 2012a, c; Schulz et al. 2011). However, the picture of (nano) confined water is still far from being complete (Giovambattista et al. 2012; Rasaiah et al. 2008; Berne et al. 2009; Schulz et al. 2011; Alarcón et al. 2014). This issue is not only crucial from an intrinsic, fundamental level, but also from its far reaching implications (Fernández 2010; Qvist et al. 2008; Berne et al. 2009; Young et al. 2007; Wang et al. 2011; Kulp III et al. 2011; Accordino et al. 2011a, 2012a, b, c, 2013; Schulz et al. 2011; Sierra et al. 2013; Alarcón et al. 2014; Bogan and Thorn 1998; Li and Liu 2009). For example, being water the matrix of life, a full understanding of its behavior in the nano and mesoscales would be essential to understand biology at the molecular level. In biological organization processes, water acts as a mediator between complex surfaces which tend to associate by means of interactions of non-covalent type (Giovambattista et al. 2012), thus generating nanoconfined environments for which our knowledge of the behavior of bulk water might be of little value. Such new settings claim for the development of a novel intuition. One such example is the nanoconfinement produced upon association of hydrophobic surfaces, which affects the thermodynamic properties of the hydration water in order to produce the “drying” process promoter of hydrophobic collapse. Another example is the binding of a ligand to a protein, which is expected to displace easily removable hydration water (Fernández and Scheraga 2003; Fernández and Scott 2003; Fernández 2010; Qvist et al. 2008; Berne et al. 2009; Young et al. 2007; Wang et al. 2011; Kulp III et al. 2011; Accordino et al. 2012a, b, c, 2013; Sierra et al. 2013; Alarcón et al. 2014; Bogan and Thorn 1998; Li and Liu 2009). Thus, the knowledge of how different nanoconfinement conditions (both of chemical and geometrical nature) affect hydrophobicity is therefore not only of great significance

to understand and to predict the behavior of these systems, but also to guide the efforts to emulate them in bioengineering. Notwithstanding this, a complete theory of hydrophobicity at the nanoscale level is still lacking (Giovambattista et al. 2012).

In turn, the principles that govern biological organization at the molecular level are the same as the ones acting in the self-assembly of molecular structures to create synthetic supramolecular nanometrically-sized materials (Giovambattista et al. 2012). The solvent therefore plays a key role in the design of new materials (Giovambattista et al. 2012; Faul and Antonietti 2003; Rehm and Schmuck 2010). Water is the natural solvent in bioengineering and drug design, but is also becoming increasingly important in supramolecular chemistry. But despite the growing importance of green chemistry, it is interesting to note that chemists (whose synthesis is predominantly organic and non-aqueous) are finding it difficult to imitate the kind of processes that Nature performs all the time (Faul and Antonietti 2003; Rehm and Schmuck 2010) (obviously, Nature has much to teach us in this regard). Also, chemical research has tried to emulate certain rules of Biology in generating nanoscale structures by working with building blocks to attain materials of greater complexity and functionality, thus distributing a complex structural and functional problem at different levels of integration (Faul and Antonietti 2003; Rehm and Schmuck 2010) (coding three-dimensional structure in chemical sequence). However, for this to be effective we should fully understand the principles that govern the interactions, generally of non-covalent nature, between such modular units operating within nanoconfined environments in which the solvent is obviously discrete and not a continuous medium. Additionally, the way in which non-covalent interactions depend on their local environment is not fully understood (Fernández and Scheraga 2003; Fernández and Scott 2003; Fernández 2010; Accordino et al. 2012a, b, c, 2013; Sierra et al. 2013). Very often concepts derived in bulk conditions or *in vacuo*, not necessarily valid under nanoconfinement conditions, are applied. Non-covalent interactions of use in supramolecular chemistry (Faul and Antonietti 2003; Rehm and Schmuck 2010), such as hydrogen bonds and ionic interactions are extremely weak and even irrelevant in bulk water given solvation and screening. However, such interactions might be strong in nanoconfined environments, where the local "effective dielectric" is diminished and coulombic interactions are strengthened (Fernández and Scheraga 2003; Fernández and Scott 2003; Fernández 2010; Accordino et al. 2012a, b, c, 2013; Sierra et al. 2013). The glaring weakness of certain non-covalent interactions in water has led to use the so-called "Gulliver principle": to add interactions of equal or different nature, as if a giant were to be tied through many tiny ropes. However, for this strategy not to still remain conceptually "Lilliputian" it should be considered that the effects of these interactions are not necessarily simply additive, while the way they depend on the local environment should be understood. This same ignorance is also observed in other contexts such as bioengineering and drug design, so the scarcity of rational design elements and the overwhelming dominance of "trial and error" attempts (expensive and suboptimal) are not surprising. Thus, it is not enough to add-up interactions but to combine them in a suitable topology. For example, the role of the local hydrophobic content around

hydrogen bonds in protein binding and drug design has been turned into a design concept (Fernández and Scheraga 2003; Fernández and Scott 2003; Fernández 2010; Accordino et al. 2012a, b, c, 2013; Sierra et al. 2013).

The above-expounded scenario is obviously extremely vast. In this chapter we do not mean to provide a comprehensive all-embracing treatment, but to focus on certain issues arbitrarily chosen by our particular interest. Thus, while we shall mainly review some recent computational work of our group, we will refer it to a generic context of wide-ranging interest. A useful introduction to this field is the investigation of the hydration properties of model systems, like simple hydrophobic-like surfaces. Such studies where geometry plays a main role can also be taken as simple first steps towards more complex situations where chemistry is also at play, like the situation encountered for the so-called biological water, that is, the hydration water around proteins and other biological molecules. Extensive hydrophobic-like surfaces disrupt the hydrogen bond network of water. In the absence of significant attractive interactions with the surface, the water molecules close to a hydrophobic surface would lack a hydrogen bond in such direction, thus diminishing their local connectivity from preferentially four to preferentially three first neighbors. In the present work we shall study by means of molecular dynamics (MD) simulations the structure and also the orientation of the water molecules at graphene surfaces, single walled carbon nanotubes of different radii and fullerenes. We shall also study the hydration of model alkane-like self-assembled monolayers (SAMs) and the filling/drying propensity of cavities and tunnels carved in the SAMs. Additionally, we shall study the hydration layers of the protein lysozyme and we shall also present some preliminary studies on hydration and water penetration in phospholipid membranes. Thus, we shall investigate both the role of curvature and chemistry on the properties of hydration water. Improved structuring as compared to the bulk will be made evident at surfaces together with clear preferential orientational ordering. The study of the orientation of the water molecules is interesting since it can be directly contrasted with experimental measurements (surface sum-frequency vibrational spectroscopy (Shen and Ostroverkhov 2006), when available. Our studies will also show the possibility of geometrically-based subnanoscale dewetting. Finally, by means of the study of water density fluctuations, we shall estimate the local hydrophobicity properties both for model surfaces and for the different groups of the lipid bilayer. These studies might be relevant for the comprehension of the behavior of binding sites in different contexts which, as already indicated, are expected to present easily removable hydration water which might be replaced by the ligand upon binding (Fernández and Scheraga 2003; Fernández and Scott 2003; Fernández 2010; Qvist et al. 2008; Berne et al. 2009; Young et al. 2007; Wang et al. 2011; Kulp III et al. 2011; Accordino et al. 2012a, b, c, 2013; Sierra et al. 2013; Alarcón et al. 2014; Bogan and Thorn 1998; Li and Liu 2009). We thus conclude with a few words of further emphasis on the relevance of this kind of knowledge to biology and to the design of new materials by highlighting the context-dependent and non-additive nature of different con-covalent interactions in an aqueous nanoenvironment, an issue that is usually greatly overlooked.

## 7.2 Hydration and Geometry

The hydration properties of a solute are not only defined by the chemical nature of the solute but also by its geometry. For example, a (very) small nonpolar solute can be clathrated by water while larger nonpolar solutes aggregate by means of the hydrophobic effect. Water molecules in the clathrate basically retain the fourfold hydrogen bond (HB) coordination typical of bulk water while extended nonpolar surfaces disrupt the HB network and thus the water molecules at the surface are engaged in less than four HBs. In turn, it has been shown that subnanometric nonpolar cavities (spherical pores) remain empty, whereas water penetrates nanometric size ones (Rasaiah et al. 2008; Schulz et al. 2011). This behavior is due to the reluctance of the water molecules to resign hydrogen bond coordination with other water molecules (only nanometric size cavities allow penetration retaining the coordination typical at surfaces). For example, the interiors of the spherical $C_{180}$ and $C_{140}$ fullerenes (the size of the last one being barely larger than 10 Å) have been shown to present stability for filled states with small clusters of water molecules connected by strong hydrogen bonds (Rasaiah et al. 2008 and references therein). Also, the filling and the conduction of water in carbon nanotubes and related systems have been extensively studied (Rasaiah et al. 2008 and references therein) and many different water phases have been discovered (from 1D trains of hydrogen-bonded water molecules at low nanotube radius to complex layered structures within larger nanotubes). It has also been shown that the hydrophobicity of the material is important since a small reduction of the van der Waals attraction between water and the carbon atoms induces the drying of previously filled nanotubes (Rasaiah et al. 2008). In addition, the behavior of water confined in cylindrical pores or tunnels is also important both from the basic and the applied viewpoints. For instance, this behavior is relevant for water flow in aquaporins and proton flow in proton pumps and enzymes (Rasaiah et al. 2008). Additionally, while it is generally believed that small protein cavities are empty (Qvist et al. 2008), there is no general consensus on whether large protein cavities are filled or empty and certain experimental results on the subject are contradictory (even when certain large cavities seem to indeed present small clusters of confined water molecules) (Rasaiah et al. 2008; Qvist et al. 2008). Thus, since in complex realistic systems both geometry and chemistry affect its hydration properties, it becomes convenient to first separate them by focusing in simple systems to study the role of geometry to then consider more realistic contexts like, for example, proteins and phospholipid membranes.

### *7.2.1 Water at Graphitic-Like Surfaces: Graphene, Carbon Nanotubes and Fullerenes. The Role of Curvature and Water Orientational Ordering*

In this section we review our computational work on model hydrophobic surfaces: a graphene sheet, single-walled carbon nanotubes of different radii and $C_{60}$ and

$C_{20}$ fullerenes (Malaspina et al. 2010; Alarcón et al. 2011; Accordino et al. 2011a, 2012a, c; Gelman Constantin et al. 2011; Schulz et al. 2011). Given the chemical similarity between the three kinds of systems under study, the hydration of the graphene sheet should constitute the limit of infinite curvature radius for both the nanotubes and the fullerenes.

The water molecules were modeled by the TIP3P. The equilibration was carried out with a canonical NVE ensemble with a Berendsen thermostat. All simulations were done using the AMBER10 molecular simulation suite with a 1 fs time step (we used the GAFF and FF99SB force fields for carbon and water, respectively). All calculations were performed in the NpT ensemble with a Langevin thermostat.

The model graphene surface was a perfect honeycomb graphite-like sheet, consisting of a layer of 5 by 5 benzenic rings (approximately 100 $Å^2$) with terminations in hydrogen atoms solvated with 4,365 TIP3P water molecules in an orthogonal cubic box with periodic boundaries. The surface was centered in the middle of the box and parallel to the XY plane. To discard the presence of significant finite size effects we also employed a second layer of 10 by 10 benzenic rings (approximately 400 $Å^2$), solvated with 10,788 TIP3P water molecules.

In order to avoid molecules close to borders of the graphene sheet, we considered a circular tube of radius 4.8 Å (8.4 Å for the larger system) placed at the center of the graphene layer and normal to such plane. We then divided the tube in six consecutive regions or cylinders (from region or cylinder 1 to region or cylinder 6) of height 3.5 Å so that the first cylinder extended from the surface to a distance of 3.5 Å, the second one went from 3.5 to 7 Å, and so on. This distance implies that the first region contained water molecules exclusively from the first peak of the water density distribution function normal to the surface. Since the system is equivalent in the two directions normal to the graphene plane, we gathered statistical data from both sides of the sheet (that is, we also constructed a tube normal to the graphene sheet but extending to the other direction and divided it into six cylinders). Thus, from now on when we speak of a given region or cylinder number it means that we are gathering data from the water molecules of the corresponding cylinders at the two sides of the graphene layer.

In turn, the single-walled carbon nanotubes employed had radii 2.0, 3.9, 4.75, 8.15, 12.25, 20.4 and 67.5 Å. Each of the nanotubes was solvated in a box of TIP3P water molecules that extended more than 20 Å away from the nanotube borders in each direction. The axis of the nanotube coincided with the x axis and the length of the nanotubes was 14 Å in all cases and thus, this dimension was always extensive. We studied the water molecules located within six concentric annular regions of 3.5 Å thickness so that the first region contained the water molecules external to the nanotube whose distance to the nanotube surface within the (y, z) plane at its corresponding x value was lower than 3.5 Å, the second region involved the molecules whose distance to the surface lied between 3.5 and 7 Å, and so on. In other words, we divided the region external to the nanotube into six concentric tubes (the first tube radius was 3.5 Å larger than that of the nanotube, the second one's radius was 7 Å larger than the nanotube, and so on) and the region defined by any

given tube excluded the molecules within all the previous ones. In all cases, the regions studied were more than 2 Å apart from the nanotube x-endings in order to avoid border effects.

Finally, the fullerenes studied were $C_{60}$ and $C_{20}$ and were centered at the center of coordinates. Both of them were also solvated in a box of TIP3P water molecules that extended more than 20 Å away from the fullerene surface. We also studied water molecules within six regions. The spherically concentric regions studied were such that the region 1 contained the water molecules external to the fullerene whose distance to its surface was less than 3.5 Å, the second one involved water molecules whose distance to the fullerene lied between 3.5 and 7 Å, and so on.

In all cases we carried simulations at a temperature of 300 K, mean pressure of 1 bar and average density around 1.0 kg/dm$^3$. We used a time step of 1 fs and a long range interaction cutoff of 8 Å with particle mesh Ewald.

Equilibration was tested by monitoring the behavior of thermodynamical properties like temperature, pressure and energy oscillations, and by dynamical properties like oscillations in the mean squared displacement of the water molecules; the equilibration times were in each case much larger than the structural relaxation time.

To characterize water structure we used the local structural index I(i, t), proposed by Shiratani and Sasai (see Shiratani and Sasai 1996, 1998; Malaspina et al. 2009, 2010; Alarcón et al. 2011; Accordino et al. 2011a, b; Appignanesi et al. 2009, for details):

For each molecule i one orders the rest of the molecules depending on the radial distance $r_j$ between the oxygen of the molecule i and the oxygen of molecule j: $r_1 < r_2 < r_j < r_{j+1} < \ldots < r_{n(i,\,t)} < 3.7\ \text{Å} < r_{n(i,\,t)+1}$ and calculates I(i, t) as:

$$I(i,t) = \frac{1}{n(i,t)} \sum_{j=1}^{n(i,t)} \left[ \Delta(j,i,t) - \overline{\Delta}(i,t) \right]^2$$

where the index i identifies a water molecule at a given time t, $\Delta(j, i, t) = r_{j+1} - r_j$, and the bar indicates that the quantity is averaged over all water molecules.

Such index is apt to be used at interfaces, at variance of other structural indices like the (tetrahedral) orientational order parameter, which we have demonstrated to be invalid at surfaces in its original form (Accordino et al. 2011a). The key observation is the existence of certain molecules which show an unoccupied gap between 3.2 and 3.8 Å in their radial-neighbor distribution for certain periods of time. Such low-density molecules are well structured and coordinated in a highly tetrahedral manner with four other water molecules. Occupancy of such gap increases the local density and distorts the tetrahedral order of the central molecule. A high value of the index I(i, t) implies that molecule i at time t has a good tetrahedral local order and low local density (and thus, a low local potential energy since it is able bind to its first four neighbors by geometrically well-shaped hydrogen bonds), while on the contrary, low values of I(i, t) indicate a molecule with defective tetrahedral order and high-local density (and thus, high local potential energy), even allowing for a fifth neighbor within the coordination shell. We have

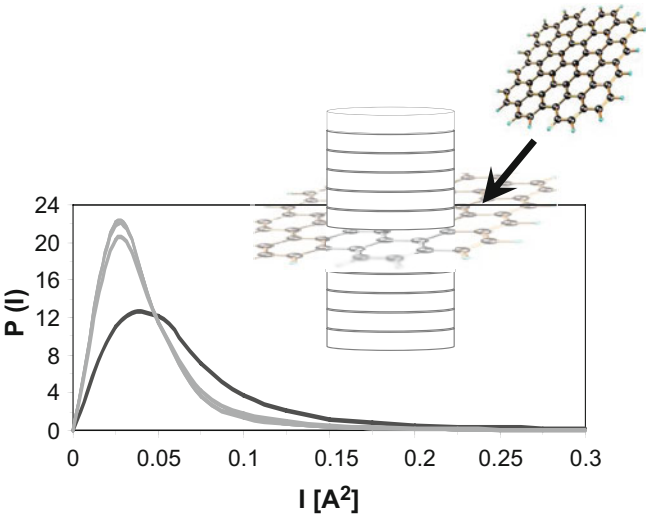


**Fig. 7.1** Scheme of the graphene sheet with the different cylinders studied and the simulation box, and the distribution of the local structure index, I, for the different cylinders studied. The *black curve* corresponds to cylinder 1. All the other cylinders display a similar behavior (only cylinder 2 shows a slightly different distribution but still far form the curve for cylinder 1)

shown that when this index is calculated for minimized water configurations (called inherent structures) it is possible to obtain clear bimodal distributions, thus speaking of the existence of low and high local density water molecules (Appignanesi et al. 2009; Malaspina et al. 2009; Accordino et al. 2011b). However, in the present work we shall directly use the real dynamics configurations without minimization.

In Fig. 7.1 we show the results for the graphene sheet. We can clearly see that the distribution of the local structure index, I, for the first cylinder is clearly displaced to the right as compared to the rest of the cylinders (the water molecules in the outermost cylinders in fact show a bulk-like behavior). This fact speaks of the better structuring of the water molecules close to the surface and that this structuring effect is only local and is quickly lost when we move away from the surface.

We obtained similar results for the exterior faces of carbon nanotubes and fullerenes: Only the water molecules close to the surface of these objects showed a better structuring than bulk water. However, we were interested in determining the effect of curvature on the structure of hydration water. To that end, we studied (as indicated above) nanotubes of different radii. We found that the structuring of the first hydration layer indeed depends on the local curvature since the structuring gets poorer as the radius of the nanotube drops. The first cylinder of the smallest nanotube and the first spherical region of the small fullerenes showed less structuring (I index distribution displaced to the left) than the first cylinder of the largest nanotube which displayed a behavior very similar to that of the first cylinder of the graphene sheet. These results are displayed in Fig. 7.2.

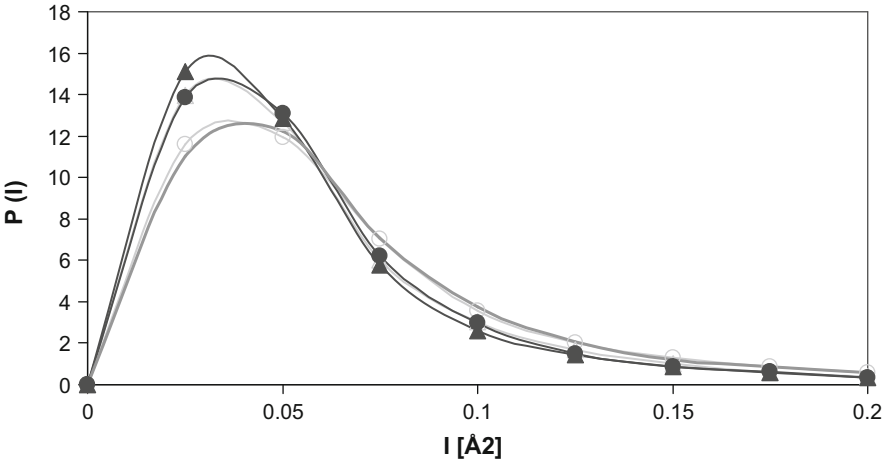


**Fig. 7.2** Distribution of the index I for the first hydration layers of the smallest and largest nanotubes, the fullerenes and the graphene sheet. *Black curves* for fullerenes (*triangles* for $C_{20}$ and *circles* for $C_{60}$), *light gray* curves for carbon nanotubes (*triangles* for small radius nanotubes and *circles* for large ones) and *dark gray curve* for the graphene sheet

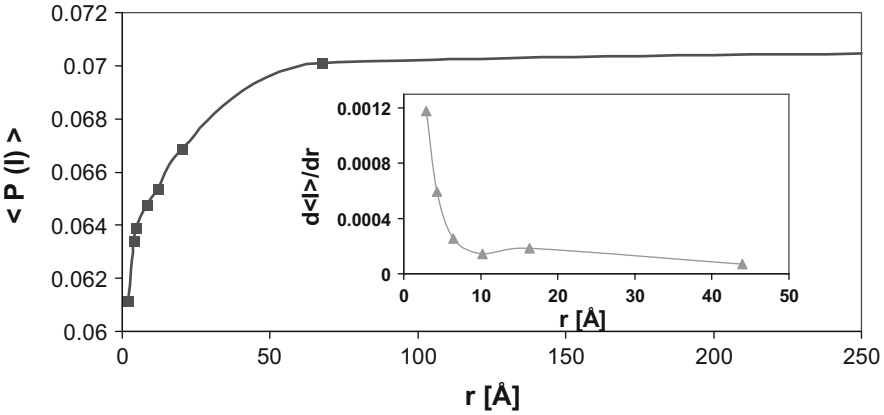


**Fig. 7.3** Mean value of the local structure index I for the water molecules in the first cylinder around carbon nanotubes as a function of the nanotube radius. *Inset*: Derivative of the former quantity

In turn, in Fig. 7.3 we show the mean value of the index I for the first hydration layer of the carbon nanotubes studied as a function of nanotube radius. From such figure we can learn on the great loss in water structure around the subnanometric regime. That is, when the diameter of the nanotube gets below the nanometer (10 Å), the structuring of the water molecules of the first hydration layer is quickly lost.

The previous results speak of an increased structural ordering of the water molecules close to graphitic-like surfaces as compared to bulk water. Now we would like to know which kind of order is being developed close to the surfaces. It is expected that the water molecules close to the surface loss a hydrogen bond in the direction towards the surface plane and would be preferentially coordinated with other three water molecules via a hydrogen bond (as compared to the 4-fould coordination typical in the bulk). It is important to notice, however, that the index I is sensitive to the quality of the first coordination sphere irrespective of the number of first neighbors. Then, we studied the distribution of water molecules with three or less hydrogen bonds (HB) and with four HBs, as a function of the distance to the surface. In so doing, we verified that the molecules close to the surface (those which most contribute to cylinder 1) are indeed hydrogen bonded to less than four other water molecules (we used a geometric criterion for HBs: O . . . O distance lower than 3.5 Å and O-H . . . O angle larger than 140°). Thus, such molecules are expected to loss a HB in the direction of the surface. We found that the distribution for molecules with three or less HBs display a peak close to 3 Å from the surface. However, the distribution of the molecules with four HBs displays a peak close to 4.5 Å from the surface. Both curves intersect at roughly 3.5 Å. Thus, for convenience, from now on we shall divide the water molecules inside the first peak of the density plot in two layers: layer 1, $L_1$, with molecules closer than 3.5 Å from the surface and which form preferentially three HBs, and layer 2, $L_2$, with molecules that extend from 3.5 Å to 4.25 Å from the surface and which tend to participate in 4 HBs.

To get a better idea of the structuring of the water molecules we now study the orientational ordering of molecules in $L_1$ and $L_2$. To that end, we calculate the angle $\theta$ between the normal to the surface and the OH vector, as schematically indicated in Fig. 7.4. In such figure we can see that molecules in $L_1$ and $L_2$ show clear orientational preferences, unlike the situation in bulk layers. In particular, $L_1$ shows a peak close to 70° while $L_2$ tends to peak around 0° and 110°. In turn, the bulk layer clearly shows no orientational preference, as expected. Such orientational ordering for the first two layers is typical of ice Ih (hexagonal ice). This speaks of the fact that the molecules close to the surface tend to loss the lower HB coordination as possible. Thus, they orient a vertex of the tetrahedron, in this case a lone pair, towards the surface and keep the other three HBs unperturbed. These molecules of $L_1$ hydrogen-bond to molecules in $L_2$ which preferentially form 4 HBs. Such arrangement is compatible with a local ice-like structure that extends for the first hydration layers. In Fig. 7.5 we show a scheme of a perfect hexagonal ice arrangement in contact with a graphene surface, indicating both $L_1$ and $L_2$ molecules.

The result of the ordering of the water molecules resembling the structure of hexagonal ice is similar to the situation at the water-vacuum or water-air interface (Shen and Ostroverkhov 2006; Fan et al. 2009) and to the situation in small water clusters (Gelman Constantin et al. 2011). However the orientation is on the other direction of the basal plane. In such cases the superficial water molecules orient an H atom towards the surface. In this case, molecules in the first layer ($L_1$, that is, the molecules closest to the interface) would tend to display an orientation of $\theta = 180°$

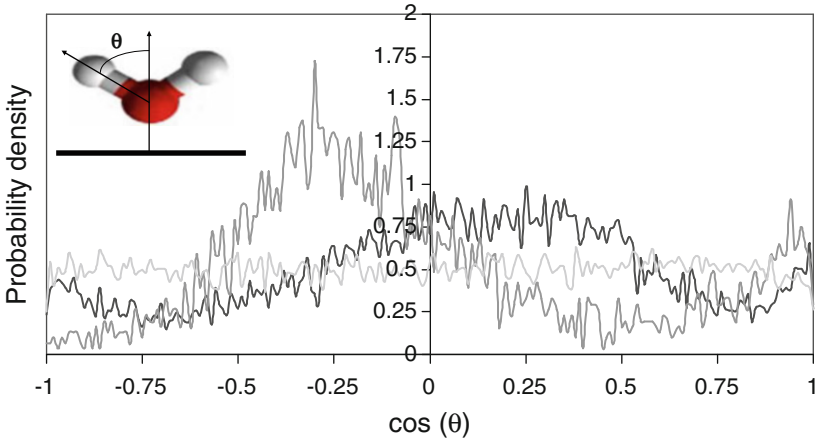


**Fig. 7.4** Distribution of the orientational angle, θ, for layer $L_1$ (*black curve*), $L_2$ (*dark gray curve*) and a bulk layer (*light gray*) for the water molecules around a graphene sheet. We have lowered temperature to T = 240 K but similar results (with less developed peaks) are seen at T = 300 K. Results are for TIP3P water, but similar results are obtained with TIP5P and SPC/E

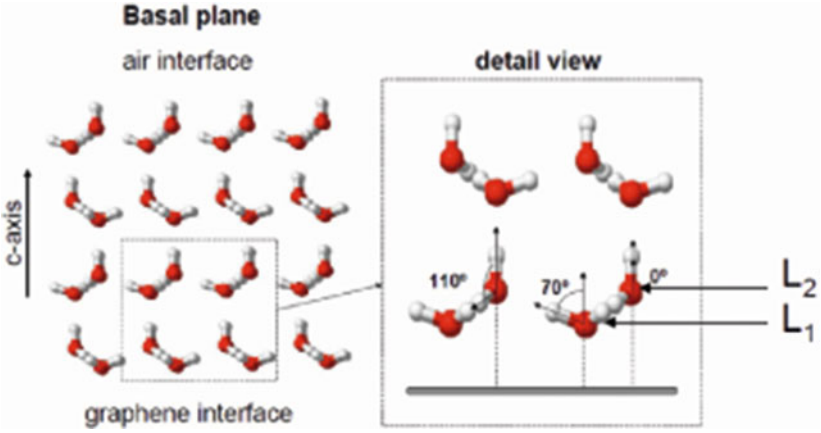


**Fig. 7.5** Scheme of a perfect hexagonal ice structure indicating the orientation the molecules tend to adopt (albeit in a more disordered fashion) over a graphene sheet. The graphene sheet would be at the bottom. At the top we place an air interface, at which the water molecules would tend to orient in the other direction along the c axis of the basal plane

and θ = 70°, while $L_2$ molecules would prefer angles of 0° and 110°. Again this situation implies a minimization of HB loss since only a vertex of the tetrahedron is lost.

Similar results are obtained for carbon nanotubes and fullerenes, with the orientational ordering getting worse as the curvature of the graphitic-like object increases.

### 7.2.2 *Water at Self-Assembled Monolayers. Filling of Cavities and Tunnels*

In order to include geometric complexity in a controlled way (as a first step towards more realistic cases like proteins and biological membranes) we study the hydration of self-assembled monolayers (SAMs) and the filling propensity of model hydrophobic pores and tunnels carved in such SAMs (for full details see Schulz et al. 2011; Alarcón et al. 2014). We note that these systems are rigid so as to preserve the desired geometry they model. Later on we shall also present some studies for flexible SAMs where water is able to penetrate and we shall also study flexible phospholipid bilayers. The SAMs studied consisted in monolayers of 81 or 144 chains (in a $9 \times 9$ or $12 \times 12$ arrangements) of n-heptadecane, $CH_3$-$(CH_2)_{15}$-$CH_3$ (in some cases we also used decane chains) aligned in a parallel fashion so as to generate a cube. This arrangement mimics the monolayer structure of stearic acid chains adopted at a water interface but replaces the acid group (COOH) by a H so that the chain ends with a methyl, i.e. it becomes a n-heptadecane chain. The original chain separation was 4.53 Å, the typical distance in a fatty acid monolayer. The monolayer was solvated with water molecules modeled by the TIP3P model with a canonical NVE ensemble with a Berendsen thermostat. All simulations were done using the AMBER10 molecular simulation suite with a 2 fs time step (we used the GAFF and FF99SB force fields). All calculations were performed in the NpT ensemble with a Langevin thermostat at $T = 300$ K. The monolayer was solvated with TIP3P water molecules in an orthogonal cubic box with periodic boundary conditions. The size of the box was such that it extended more than 20 Å away from all the monolayer faces. The surface monolayer was centered in the middle of the box. For the cavities, we carved holes in the monolayer surface parallel to the (x, y) plane in the z direction (the positions of the hydrogens at the top of the monolayer was $z = 42.5$ Å while the corresponding carbon atoms were placed at $z = 41.6$ Å. In all cases (perfect monolayer or with the different carved holes) the AMBER equilibration reduced the distance between the n-heptadecane molecules (the chain separation) to 4.2 Å.

To study the effect of concavity on hydrophobicity, we carved several cavities on the hydrophobic SAMs. This geometrical setting is of particular interest given the situations found in protein pockets and in pores at different materials. To generate the cavities we carved squared holes of different sizes at the center of the monolayer surface by cutting the corresponding number of chains (the bonds of the carbon atoms at the bottom of the hole were saturated so that all chains ended with a methyl group; in other words, they became shorter chain alkanes). Among other cases, we studied holes created when we cut 1, 4, 9, 16, 25, 36, 49 and 64 central chains in order to generate square holes of width 8.5, 12.7, 16.5, 21.3, 25.1, 29.5, 33.8 and 38.0 Å respectively (the width represents the diameters of the hole "mouth", L). Figure 7.6 shows the cases of the holes when we cut 1 chain (width of the hole equal to 8.5 Å) and 25 chains (with a size of 25.1 Å). In all cases, the chains were cut in 5 units, so that the depth of the holes was always of 6.4 Å. We mention

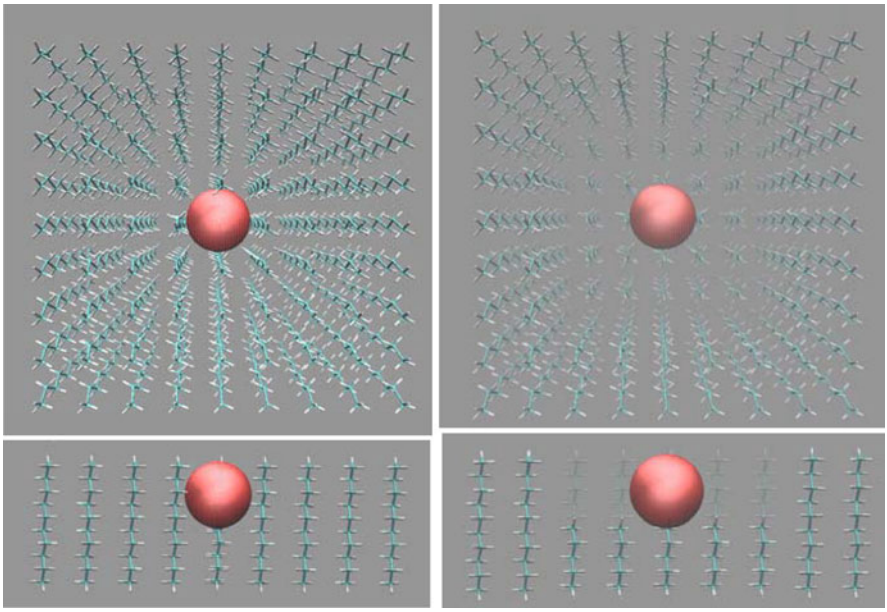

**Fig. 7.6** *Left figure*: illustration of the SAM with a hole of width 8.5 Å, where one chain (the central chain) has been shortened in 5 units to create the pore. *Top*: top view of the alkane-like monolayer; *Bottom*: side view of the monolayer, which we have cut at the middle in order to better display the hole. *Right figure*: idem but for the hole created by shortening all the central 25 chains in five units. *Top*: top view. *Bottom*: side (cut) view. The central chains, which were shortened so as to generate the hole, are shown in *light gray*. The *red sphere* indicates the observation volume used

that in order to maintain the shapes of the holes, we restricted positions for all backbone carbon atoms of the chains after equilibration. To study water penetration and hydrophobicity, we calculated the probability distributions for observing N water molecules within spheres located at the "mouth" of the different holes. This means that the observation spheres were located inside the hole, almost tangent to the line defined by the H atoms of the methyls of the alkylic chains framing the holes. Additionally, all spheres were also placed at the center of the corresponding segment that defines the top of each hole. In Fig. 7.6 we indicate the placing of the observation volumes.

We also created tunnels by using a similar procedure and thus we extracted complete chains from the center of the monolayer, so that both the upper and lower faces of the monolayer cube were connected by the tunnel. For comparison, we also simulated single-walled carbon nanotubes with radii 2.0, 3.9, 4.75, 8.15, 12.25, 20.4 and 67.5 Å. Each of the nanotubes was solvated in a box of TIP3P water molecules that extended more than 20 Å away from the nanotube borders in each direction. The axis of the nanotube coincided with the x axis and the length of the nanotubes was 14 Å in all cases.

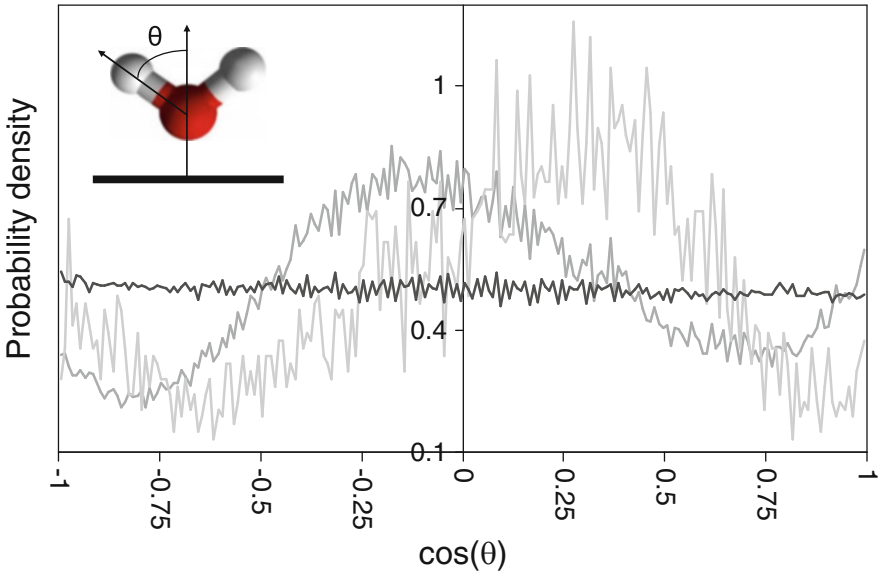


**Fig. 7.7** Orientational ordering of water molecules. *Light gray curve* for graphene surface, *dark gray curve* for the alkane-like SAM without hole and *black line* for bulk water

We first studied the orientational ordering of the water molecules at the first peak of the density plot above a perfect SAM (that is, a SAM without a hole). We note that since the SAMs are modeled by using restraints in the heavy atoms, the chains are rigid and water does not penetrate between them. Thus, hydration can be defined at a plane outside the SAM. The results are shown in Fig. 7.7. As in the case of graphene, we can also notice a clear preferential orientation of the water molecules. However, at variance from such case, the water molecules tend to display an angle between 100° and 110°, and thus they tend to orient a face of the tetrahedron parallel to the SAM surface.

In turn, Fig. 7.8 depicts the probability distributions for observing N water molecules within the spherical observation volumes for the different holes. We also include the situation for the perfect monolayer (without hole), where the sphere is located tangent to the surface. From such figure we can learn that the degree of hydrophobicity strongly depends on curvature. The holes are more hydrophobic than the perfect monolayer, but the role of geometry is more conspicuous as the hole size (the diameter of the hole "mouth", L) approaches the subnanometric regime. Such subnanometric-sized holes do not fill with water given the reluctance of the water molecules to lose their hydrogen bond coordination in order to penetrate. Larger holes (up to roughly $L = 25$ Å), where the water molecules can enter retaining their coordination, are nonetheless more hydrophobic than the perfect monolayer, which means that hydrophobicity is clearly curvature-dependent for concave surfaces. Such result of a geometrically-induced dehydration is interesting, for example, for

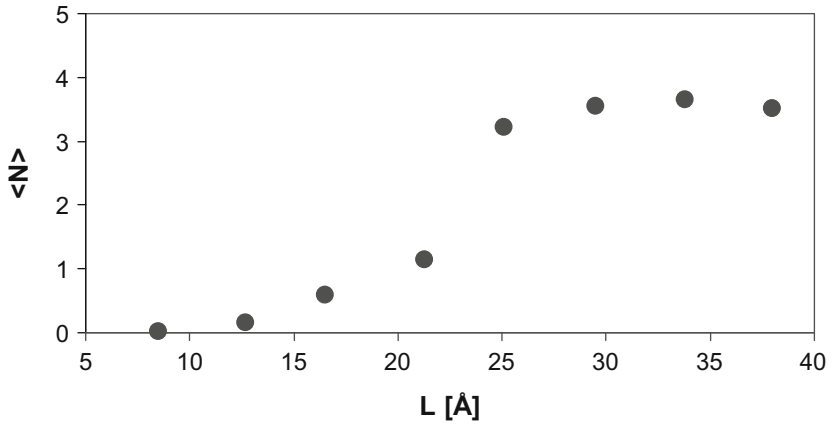


**Fig. 7.8** Mean value of the number of water molecules inside the observation volume for the different holes of size L

the context of protein binding, since protein binding pockets are expected to be dry or to contain easily removable water which should be displaced by a ligand upon association (Fernández and Scheraga 2003; Fernández and Scott 2003; Fernández 2010; Qvist et al. 2008; Berne et al. 2009; Young et al. 2007; Wang et al. 2011; Kulp III et al. 2011; Accordino et al. 2012a, b, c, 2013; Sierra et al. 2013; Alarcón et al. 2014; Bogan and Thorn 1998; Li and Liu 2009).

The results of some of these studies also enabled us to demonstrate that the filling of small nanometric cavities (Schulz et al. 2011) is not homogeneous in time but represents a dynamic process with alternation of filled and completely dry states. This is so since the water molecules inside the hydrophobic pore are able to establish some HB interactions but when an interaction is broken it cannot be compensated by other neighboring molecules like in bulk water (where the HB network is continuously rearranging given the many different possible configurations). This fact destabilizes the filling configuration and the pore is desorbed until new water penetration allows a new HB network arrangement inside the cavity. Another interesting result we obtained (Schulz et al. 2011) was that the tunnels carved in the SAMs remain empty until about twice the minimum diameter for a carbon nanotube to get filled (13.5 Å vs. 7.0 Å), thus making evident the more hydrophobic nature of such systems. In fact, the water-wall attractions play a role in the filling of carbon nanotubes, since simulations have shown that the quenching of such interactions induce drying of previously filled nanotubes (Rasaiah et al. 2008). Another feature typical of hydrophobic confinement that we have confirmed in the filling of the tunnels is that the water molecules inside them tend to be engaged in extensive HB networks where the water molecules retain a number of HB partners similar to that at the bulk. Narrower tunnels would demand a restriction in the number of HB partners which prevents them from filling.

## 7.3 Realistic Contexts. Hydration at Settings with Complex Geometry and Chemistry

Having studied simple systems with different geometries, we now turn to more realistic, complicated systems. A previous step could have been to deal with model systems with simple geometry and controlled chemical topologies, with hydrophilic and hydrophobic regions. This approach has already been taken, as can been seen in the excellent works of the groups of P. G. Debenedetti (Giovambattista et al. 2008, 2012) and S. Garde (Rasaiah et al. 2008) to which we refer the interested reader. Instead, here we shall directly tackle some aspects of the hydration of complex systems of great interest: proteins and membranes.

### *7.3.1 Protein Hydration Water*

In this section we review our work on the behavior of the hydration layers of a protein surface (Accordino et al. 2011a, 2012a, c), a lysozyme molecule, as compared with the behavior at the homogeneous hydrophobic surface of a graphene sheet. In this case the water molecules were modeled by the TIP5P model. We also modeled the water molecules in contact with a graphene sheet by means of the TIP5P model, obtaining very similar results to that of the previous section. Equilibration was carried out in two steps: In a first step we brought the system to the corresponding temperature value with a Langevin thermostat with 0.2 ps timestep and using the SHAKE algorithm; then, we performed a larger equilibration within the NpT ensemble, also using a Langevin thermostat with 2 fs timestep and the SHAKE algorithm. All simulations were done with the AMBER 10 molecular simulation suite and were performed in the NpT ensemble with a Langevin thermostat and by using a long-range-interaction cutoff of 8 Å. We simulated an orthorhombic form of hen egg-white lysozyme (Accordino et al. 2012a, c) placed within a box of 12600 TIP5P water molecules. The force field used in the simulation was ff99SB. We carried simulations at different temperatures (within the normal liquid and supercooled regimes), mean pressure of 1 bar and average density around 1.0 kg/dm$^3$.

The protein-water radial distribution function (Accordino et al. 2012a, c) presents two well-developed peaks followed by less developed structure. The first small peak corresponds to water molecules very close to the protein which form hydrogen bonds with it. We shall call these molecules as layer 1 molecules, $L_1$. In order to get a better idea on the arrangement of the molecules of the second peak, we studied the distribution of minimum distances to any atom of the protein of the hydration water molecules of the second peak of the radial distribution function by discriminating between molecules with three and four water-water HBs. The situation is somehow similar to that found for the graphene sheet with two distributions that intersect roughly at a distance of 3 Å. Thus, we again shall distinguish two layers, in this case

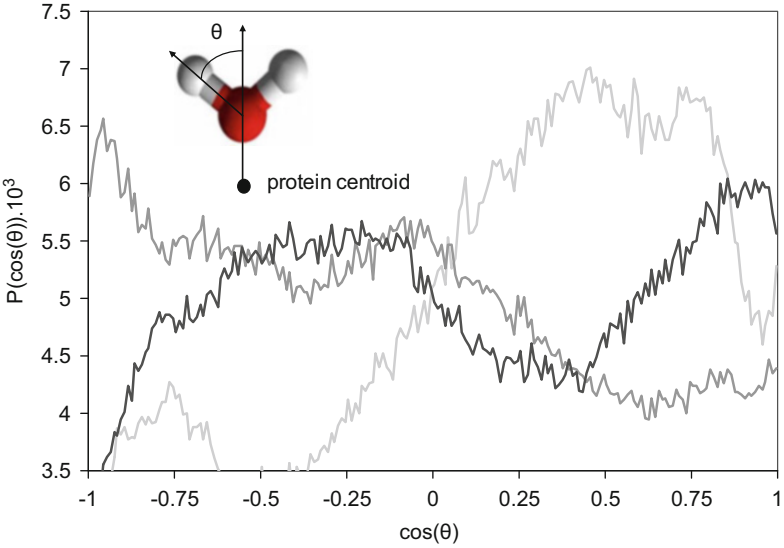


**Fig. 7.9** Orientational ordering of the water molecules in the first three layers around the lysozyme molecule. *Light gray*, *dark gray* and *black curves* represent layers 1, 2 and 3 respectively

layer 2, $L_2$, and layer 3, $L_3$. In summary, we classify the hydration water molecules in layers: $L_1$ goes from 0 to 0.2125 Å from the protein, $L_2$ goes from this value to 3 Å and $L_3$ includes molecules between 3 and 4.25 Å.

In Fig. 7.9 we show the orientational ordering of the water molecules by calculating the angle θ between the OH and the vector joining the protein centroid and the O atom of the water molecule. While lacking the neat peaks found for the graphene sheet, this figure clearly still exhibits orientational preferences. Even when the situation is more complicated than that at the graphene sheet or the water-air interface, peak positions similar to such both contexts still hold, which again speaks of certain tendency to local ice-like orientation. Hydrophobic portions of the protein are expected to present such local preferences by orienting a vertex of the tetrahedron towards the protein so as to minimize the water-water HB loss. Also when the water molecule hydrogen bonds to the protein it should orient a vertex of the tetrahedron, a situation also consistent with a local orientation similar to an ice surface. Thus, the geometric and chemical complexity does not alter significantly the local orientational preferences found in more simple contexts.

### *7.3.2 Membrane Hydration*

There is mounting evidence (Disalvo et al. 2008, and references therein; see also Arsov 2015; Nickels and Katsaras 2015; Pfeiffer 2015) for the presence of water

molecules within phospholipid membranes not only hydrating the polar lipid head groups but also buried within the apolar alkyl chains. This means that (at variance from the simple case of the rigid model SAMs we have previously studied) water penetrates the lipid bilayer towards the region of the carbonyl groups. In turn, the lipid chains are flexible molecules whose dynamics may present different conformational changes. Thus, these systems are expected to evidence a rich behavior for hydration and nanoconfined water.

To learn on the behavior of water at the water-membrane interface we simulated by means of AMBER12 package a Dipalmitoylphosphatidylcholine (DPPC) bilayer. The bilayer was composed of 128 DPPC molecules (64 per monolayer in a $8 \times 8$ arrangement). The initial separation between DPPC was 9 Å in a triangular arrangement. The temperature was 323 K (50 °C) and we solvated with a total of 10443 TIP3P water molecules (which means that we had around 81 water molecules per lipid) in order to assure that the system was fully hydrated. We solvated along the Z axis and the system was subject to periodic boundary conditions along the (X, Y) plane. Figure 7.10 shows a typical equilibrated configuration.

All the atoms of the bilayer were fixed during minimization and temperature and pressure stabilization. Then, all restraints were removed and the bilayer was free to establish a lipid-lipid equilibrium distance (we also used a more restricted system where during equilibration we fixed the positions of the last carbon atoms of the lipid tail). After 50 ns equilibration, we obtained an area per lipid of 60.3 for the free bilayers (while this distance was 65.5 Å for the system with anchored tails), a result consistent with experimental values (Nagle and Tristram-Nagle 2000). Figure 7.11 shows the time evolution of the area per lipid.

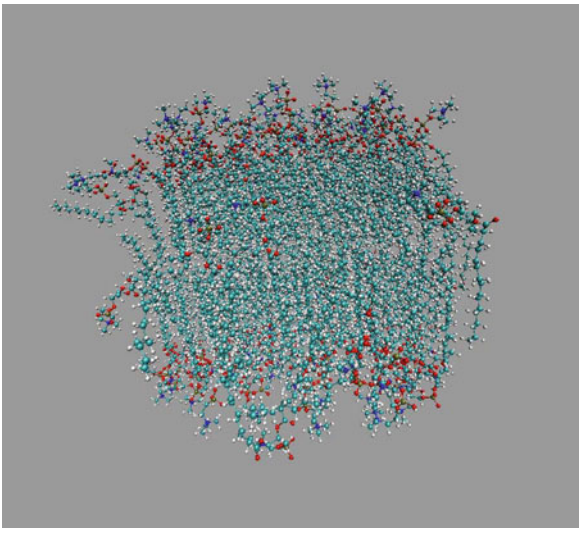

**Fig. 7.10** Image of the free bilayer. For the sake of clarity, the water molecules are not shown

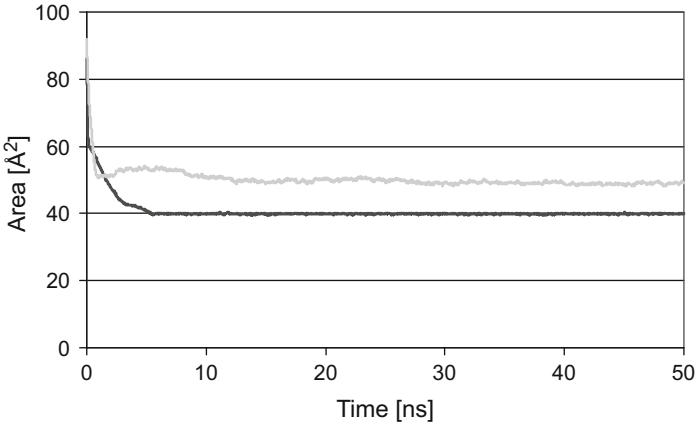


**Fig. 7.11** Time evolution of the area per lipid during stabilization

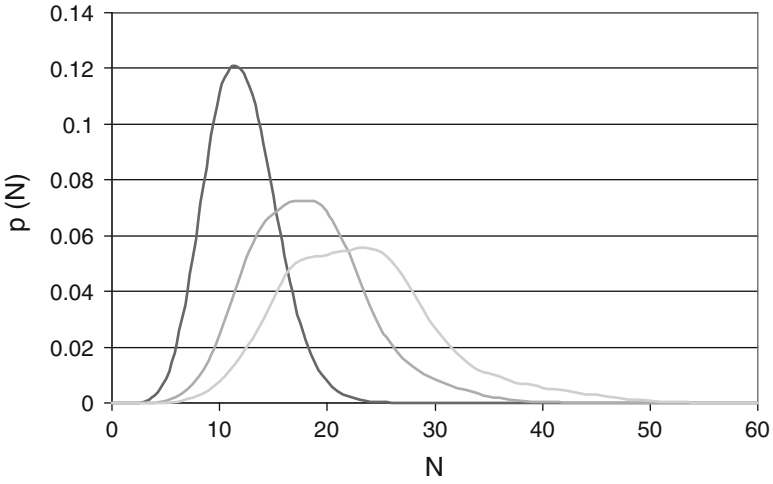


**Fig. 7.12** Distribution of the number of water molecules per lipid for threshold values of 3.5, 4.0 and 4.5 Å

Having equilibrated the free bilayers we then proceeded to calculate the number of water molecules per lipid. This was performed by counting all the water molecules whose distance to the lipid is lower than certain threshold value. We choose this value to be 4.0 or 4.5 Å in order to consider only molecules within the first hydration shell. This procedure includes molecules hydrating the exposed polar heads and also water molecules that have penetrated the bilayer. In Fig. 7.12 we present the distribution of the number of water molecules per lipid.

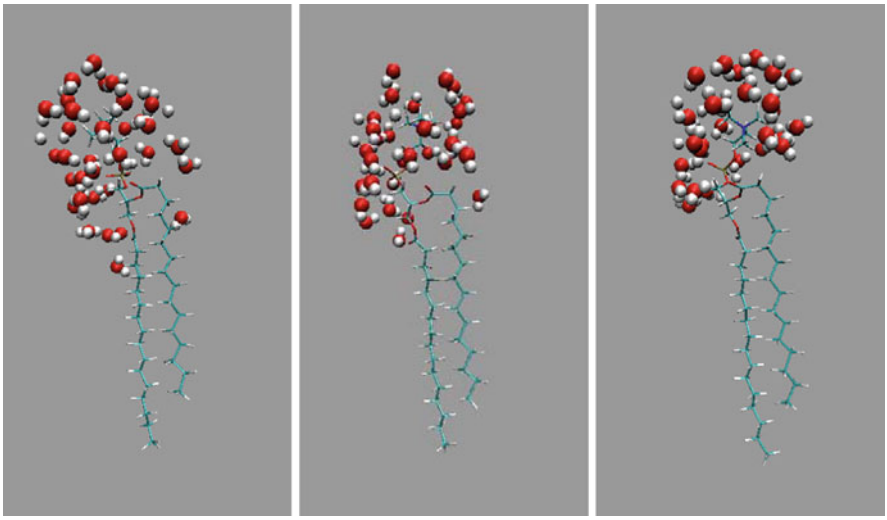

**Fig. 7.13** Examples for the location of the water molecules closest than 4.0 Å to a given lipid chain in three different configurations. For simplicity we neither display the rest of the lipid chains nor the rest of the water molecules

For the threshold of 4.0 Å the number of water molecules per lipid is 18.3, while it amounts to 23.2 when such threshold is increased to 4.5 Å. These values are consistent with experimental findings (Cevc 1987).

In turn, in Fig. 7.13 we provide examples of the spatial location of the water molecules around a selected lipid chain. We can see that the water molecules do not only hydrate the polar moieties of the chain head, but also some of them penetrate deeper the bilayer and approach the upper hydrocarbon groups.

Next, we study how these water molecules distribute among the different groups of the lipid chain. To this end, we placed a sphere of radius 4 Å centered at different heavy atoms of the lipid chain where water displays significant population. Figure 7.14 displays the results, which indicate that the phosphate oxygens Op1 and Op2 are the moieties with a higher level of hydration. The amine C atoms are also shown to be highly hydrated. In turn, the C1 and C2 atoms are also well populated by water molecules while the rest of the places display a lower level of hydration. The shapes of the curves are also instructive. Such simple featureless distributions indicate that the conformations adopted at different times are equivalent in which respects to their hydration properties. For example, if a group alternated between two different hydration states at different times, between an exposed and a buried state, the distribution would present clear signs of bimodality. This is not the case for the different groups studied.

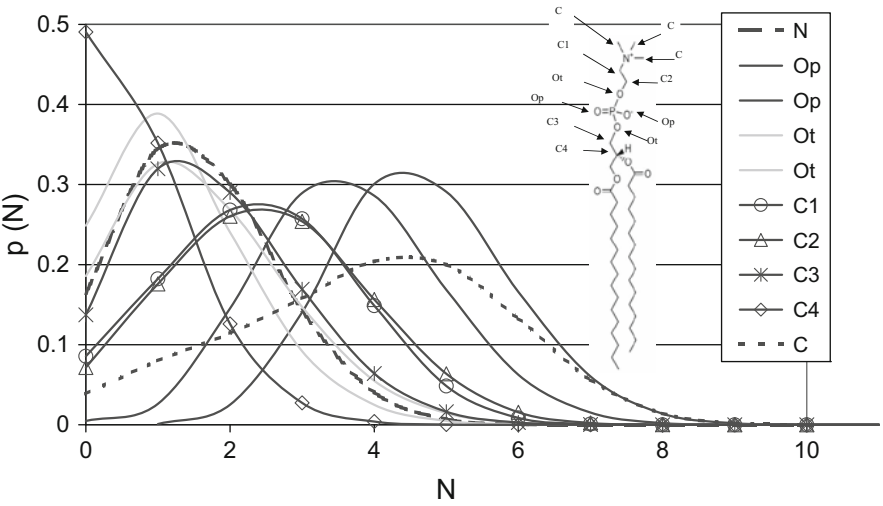


**Fig. 7.14** Distribution of water molecules around different groups of the phospholipid

## 7.4 Quantifying Local Hydrophobicity: Calculations of Water Density Fluctuations

The nanoconfinement that arises upon the interaction of different assembling units, both in biological organization processes and in the supramolecular self-assembly of nanomaterials in a water environment, affects the thermodynamic properties of the hydration water which should be removed for the process to take place (Giovambattista et al. 2012). In realistic contexts, both chemistry and local geometry are expected to define the local hydrophobicity (Giovambattista et al. 2012). Geometrically-induced surface dehydration (by means of water inaccessibly cavities) has been shown to be central for the existence of reactive sites responsible for protein binding (Schulz et al. 2011; Sierra et al. 2013). Such structural packing defects characterized by regions of the protein backbone exposed to the solvent has been shown to promote their local dehydration and to signal binding sites (Fernández and Scheraga 2003; Fernández and Scott 2003; Fernández 2010; Accordino et al. 2012a, b, c, 2013; Sierra et al. 2013). Different approaches have indicated that the hydration properties of protein binding sites play a main role in the binding of ligands or in protein-protein association (Fernández and Scheraga 2003; Fernández and Scott 2003; Fernández 2010; Qvist et al. 2008; Berne et al. 2009; Young et al. 2007; Wang et al. 2011; Kulp III et al. 2011; Accordino et al. 2012a, b, c, 2013; Sierra et al. 2013; Alarcón et al. 2014; Bogan and Thorn 1998; Li and Liu 2009). Ligands are expected to displace hydration water molecules from their binding site and the replacement of so-called “unfavorable” waters by groups of the ligand complementary to the protein surface has been established as a principal

driving force for binding (Fernández and Scheraga 2003; Fernández and Scott 2003; Fernández 2010; Qvist et al. 2008; Berne et al. 2009; Young et al. 2007; Wang et al. 2011; Kulp III et al. 2011; Accordino et al. 2012a, b, c, 2013; Sierra et al. 2013; Alarcón et al. 2014; Bogan and Thorn 1998; Li and Liu 2009). In fact, this description has been shown to hold valid for a significant fraction of receptors of pharmaceutical interest (Berne et al. 2009; Young et al. 2007; Wang et al. 2011). Even in some cases, a portion of the receptor active site is so unfavorable for water molecules that it tends to remain practically dry (Berne et al. 2009; Young et al. 2007; Wang et al. 2011). Thus, the estimation of the free energy contribution involved in the displacement of quasilocalized water molecules with unfavorable free energies in the receptor active site constitutes an issue of great interest in computational structure-based drug design (Berne et al. 2009; Young et al. 2007; Wang et al. 2011). Within this same philosophy (Kulp III et al. 2011), a study of fragment clustering of diverse organic probes on hen egg white lysozyme combined with water exclusion (superimposing the different regions targeted by the fragments with the map of water molecules tightly bound to the protein which excluded by blocking possible target regions) has been able of predicting the experimentally known binding site, or hot spot. Thus, a picture of protein binding with regions of easily removable (non-tightly-bound) water molecules at small-molecule binding sites or protein-protein interaction hot spots is emerging. Hence, it becomes relevant to develop a quantitative measure of hydrophobicity useful in determining such regions.

Amongst the different structural, dynamical and thermodynamical measures of hydrophobicity which have been proposed (Giovambattista et al. 2012; Rasaiah et al. 2008), a very appealing one consists in the quantification of water density fluctuations (Rasaiah et al. 2008). It has been demonstrated that superficial water density profiles do not represent a good measure of surface hydrophobicity. This can be expected in terms of the usual knowledge that water abhors vacuum and thus, water molecules tend to hydrate both polar and nonpolar surfaces and, thus, the density profiles normal to the surface plane display similar characteristics, with layering structure in both cases. However, at variance form hydrophilic surfaces where the water molecules are subject to significant attractive interactions, interactions are very weak at hydrophobic surfaces, which makes the hydrating water molecules to display low residence times and to become easily removed. Thus, such hydration layers display enhanced dynamics (Giovambattista et al. 2012; Rasaiah et al. 2008) enhanced compressibility (Giovambattista et al. 2012; Rasaiah et al. 2008) and enhanced density fluctuations (Rasaiah et al. 2008). In particular, the density fluctuations at differently functionalized self-assembled monolayers (SAMs) have been characterized demonstrating that hydrophobic-like surfaces do in fact present much larger density fluctuations than the ones displayed by hydrophilic-like surfaces, thus providing a good quantitative measure of hydrophobicity (Rasaiah et al. 2008). Normalized fluctuations of water number density, $\sigma^2/<N>^2$ in small observation volumes (where N is the number of water molecules within such volume) are approximately equal to $2\mu^{ex}/kT$, where $\mu^{ex}$ is the free energy of formation of cavity of such radius (Rasaiah et al. 2008). Thus,

a high value of the normalized density fluctuations at a given place indicates a favorable work of cavity creation at such place and, thus, a high hydrophobicity. The relevance of this measure is obvious from the above-described scenario: The self-assembling process of nonpolar solutes in water makes use of such dehydration propensity properly accounted for by the density fluctuations measurements, while the binding sites of proteins also exploit this phenomenon since ligands are expected to displace easily removable hydration water upon binding.

We have calculated water density fluctuations at model surfaces, functionalized SAMs, phopholipid membranes and are also studying protein binding sites. In which follows we present some preliminary results. For comparison, we calculated density fluctuation on self-assembled alkane-like monolayers like the ones of Sect. 7.2.2, but functionalized in order to be hydrophobic or hydrophilic. To this end, the chain heads consisted of $CH_3$ groups or OH groups respectively. At variance from the previous situation where the alkyl chains were rigid, here the chains are flexible. Additionally, differently from previous studies and in order to compare with the situation at the different groups of the phospholipid membranes of Sect. 7.3.2, we calculate water density fluctuations within spheres centered at the heavy atoms of the groups of interest. Thus, such observation volumes move with the atom, being appropriate for studies on flexible molecules. In Fig. 7.15 we display the probability distributions for observing N water molecules, p(N), within a small spherical observation volume of radius 4.0 Å centered at the C of the methyl heads of the hydrophobic SAMS, at the O of the alcohol head groups of the hydrophilic SAMS and at different heavy atoms of the head groups of the phospholipid membranes. A high probability of having zero water molecules in the observation domain, and thus a high value of density fluctuations, implies an enhanced propensity for dehydration or high hydrophobicity. From direct inspection of such figure, we can learn that the phosphate oxygens Op are the most hydrophilic moieties of the lipid bilayer with a hydrophilicity similar (or even higher) to the hydrophilic SAM. The C4 carbons are the most hydrophobic groups presenting density fluctuations similar to the ones of the hydrophobic SAM, while the rest of the groups display an intermediate behavior. As evident from such figure, the different oxygens present behaviors that vary from each other, as also happens for the comparative behavior of different carbonaceous groups. A first lesson emerging from this study is, thus, that the hydrophobicity of a given group can vary significantly depending on its local environment, where both the local chemistry and geometry can play a role. This fact is relevant, for example, for the behavior of binding sites. We are at present performing studies of this kind in protein binding sites. It is known that some binding sites present reactive groups surrounded by (hydrophobic) groups that can locally dehydrate the binding site, as in the O-Ring theories (Bogan and Thorn 1998; Li and Liu 2009). Electrostatic interactions (like hydrogen bonds and ionic interactions) might be strongly enhanced within an environment with a deprived local dielectric given the shielding effect of nonpolar groups (Fernández and Scheraga 2003; Fernández and Scott 2003; Fernández 2010; Accordino et al. 2012a, b, c, 2013; Sierra et al. 2013). Thus, the combination of different non-covalent interactions can produce clearly non-additive effects.

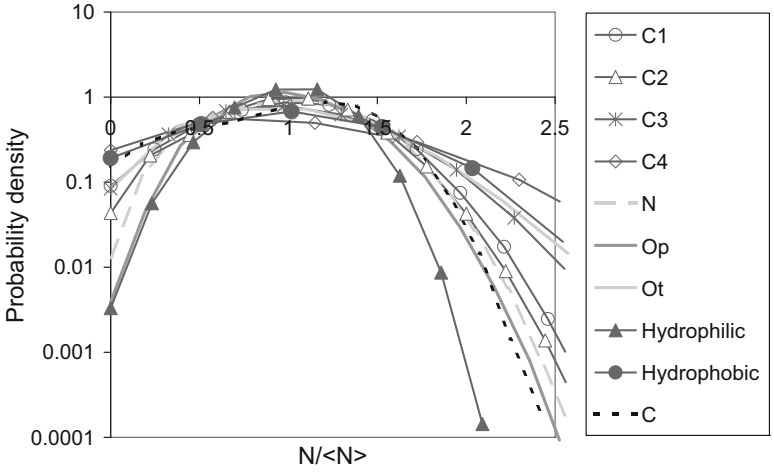


**Fig. 7.15** Probability distributions for observing N water molecules, p(N), within a small spherical observation volume of radius 4.0 Å centered at the C atoms of the methyl heads of the hydrophobic SAMS (*black line* and *black triangles*), at the O of the alcohol head groups of the hydrophilic SAMS (*black line* and *black circles*) and at different heavy atoms of the head groups of the phospholipid membranes

## 7.5 Conclusions and Future Directions

Our study of the hydration layers of different nonpolar surfaces has made evident the existence of an enhancement of water structuring at interfaces. The water molecules present a neat orientational ordering, in some cases resembling an ice-like arrangement. Inclusion of curvature induces a loss in the water structuring. The water molecules tend to exclude the hydrophobe with a minimum loss in HB coordination. Thus, they tend to orient a vertex of the tetrahedron hence conserving the other three first neighbors largely unperturbed. A more complex example, the protein lysozyme still partially displayed this behavior.

We have also shown that subnanometric size cavities carved in hydrophobic SAMs remain "dry", while intermediate size cavities exhibit an alternation of filled and dry states. These facts can be explained in terms of the reluctance of the water molecules to loss HB coordination. The degree of hydrophobicity of the material is also important since small radius carbon nanotubes can be filled while the more hydrophobic alkane-like tunnels of similar size still remain dry. We have also shown that the formation of an extensive HB network is required for filling to occur.

Some preliminary results have also been presented on the hydration and water penetration in phospholipid membranes. We have studied the spatial distribution of water molecules around the different groups of the lipid molecules of the bilayer. Water density fluctuation calculations have also enabled us to test the hydrophobicity of the different moieties.

These results are first steps in a systematic effort to learn how geometry and chemistry affect hydrophobicity and the behavior of nanoconfined water. This knowledge is expected to be relevant for the understanding of biological organization and for supramolecular self-assembly in materials science. In such processes, the nanoconfinement that arises upon the interaction of the different assembling units affects the thermodynamic properties of the hydration water, which usually must be removed for the process to take place. In such contexts, bulk-like knowledge could be not only useless but also misleading and thus a new intuition and new principles are necessary. In this light, it is not surprising that today rational design is practically absent in fields ranging from drug design to the design of soluble self-assembled materials. Most of the non-covalent interactions (mainly the ones which are electrostatic in nature) invoked in such fields would not be operative in bulk water conditions. However, the different non-covalent interactions (like HBs, ionic interactions and hydrophobic interactions) can be clearly non-additive under nanoconfinement, a context-dependent nature which is usually overlooked in design efforts. Thus, a more complete knowledge of the behavior of water under nanoconfinement is expected to open new roads of both academic and technological relevance.

**Acknowledgements** LMA, JAR-F, MBS, MAM and GAA are research fellows of CONICET. SRA and JMM-O thank CONICET for a fellowship. The authors gratefully thank CONICET and MinCyT for financial support.

## References

Accordino SR, Malaspina DC, Rodríguez Fris JA, Appignanesi GA (2011a) Comment on "Glass transition in biomolecules and the liquid-liquid critical point of water". Phys Rev Lett 106:029801

Accordino SR, Rodriguez Fris JA, Sciortino F, Appignanesi GA (2011b) Quantitative investigation of the two-state picture for water in the normal liquid and the supercooled regime. Eur Phys J E 34:48

Accordino SR, Malaspina DC, Rodriguez Fris JA, Alarcón LM, Appignanesi GA (2012a) Temperature dependence of the structure of protein hydration water and the liquid-liquid transition. Phys Rev E 85:031503

Accordino SR, Morini MA, Sierra MB, Rodríguez Fris JA, Appignanesi GA, Fernández A (2012b) Protein packing defects "heat up" interfacial water. Proteins Struct Funct Bioinf 80:1755

Accordino SR, Rodriguez Fris JA, Appignanesi GA, Fernández A (2012c) A unifying motif of intermolecular cooperativity in protein associations. Eur Phys J E 35:59

Accordino SR, Rodriguez Fris JA, Appignanesi GA (2013) Wrapping effects within a proposed function-rescue strategy for the Y220C oncogenic mutation of protein p53. PLoS One 8, e55123

Alarcón LM, Malaspina DC, Schulz EP, Frechero MA, Appignanesi GA (2011) Structure and orientation of water molecules at model hydrophobic surfaces with curvature: from graphene sheets to carbon nanotubes and fullerenes. Chem Phys 388:47

Alarcón LM, Montes de Oca JM, Accordino SR, Rodriguez Fris JA, Appignanesi GA (2014) Hydrophobicity and geometry: water at curved graphitic-like surfaces and within model pores in self-assembled monolayers. Fluid Phase Equilib 362:81

Appignanesi GA, Rodríguez Firs JA, Sciortino F (2009) Evidence of a two-state picture for supercooled water and its connections with glassy dynamics. Eur Phys J E 29:305
Arsov Z (2015) Chapter 6: Long-range lipid-water interaction as observed by ATR-FTIR spectroscopy. In Disalvo EA (ed) Membrane hydration: the role of water in the structure and function of biological membranes. Springer, Cham, pp 127–159
Berne BJ, Weeks JD, Zhou R (2009) Dewetting and hydrophobic interaction in physical and biological systems. Annu Rev Phys Chem 60:85
Bizzarri A, Cannistraro SJ (2002) Molecular dynamics of water at the protein-solvent interface. Phys Chem B 106:6617
Bogan AA, Thorn KS (1998) Anatomy of hot spots in protein interfaces. J Mol Biol 208:1
Cevc G (1987) How membrane chain melting properties are controlled by the polar surface of the lipid bilayers. Biochemistry 26:6305
Choudhury N, Montgomery PB (2005) Dynamics of water trapped between hydrophobic solutes. J Phys Chem B 109:6422
Disalvo A, Lairion F, Martini F, Tymczyszyn E, Frias M (2008) Structural and functional properties of hydration and confined water in membrane interfaces. Biochim et Biophys Acta (BBA)-Biomembranes 1778:2655
Fan Y, Chen X, Yang L, Cremer PS, Gao YQ (2009) On the structure of water at the aqueous/air interface. J Phys Chem B 113:11672
Faul CFJ, Antonietti M (2003) Ionic self-assembly: facile synthesis of supramolecular materials. Adv Mater 15:673
Fernández A (2010) Transformative concepts for drug design: target wrapping. Springer, Heidelberg
Fernández A, Scheraga HA (2003) Insufficiently dehydrated hydrogen bonds as determinants of protein interactions. Proc Natl Acad Sci U S A 100:113
Fernández A, Scott R (2003) Adherence of packing defects in soluble proteins. Phys Rev Lett 91:018102
Gelman Constantin J, Rodriguez Fris JA, Appignanesi GA, Carignano MA, Szleifer I, Corti HR (2011) Structure of supercooled water in clusters and bulk and its relation to the two-state picture of water: results from the TIP4P-ice model. Eur Phys J E 34:126
Giovambattista N, Debenedetti PG, Lopez CF, Rossky PJ (2008) Hydrophobicity of protein surfaces: separating geometry from chemistry. Proc Natl Acad Sci U S A 105:2274
Giovambattista N, Rossky PJ, Debenedetti PG (2012) Computational studies of pressure, temperature and surface effects on the structure and thermodynamics of confined water. Annu Rev Phys Chem 63:179
Huang DM, Chandler D (2000) Temperature and length scale dependence of hydrophobic effects and their possible implications for protein folding. Proc Natl Acad Sci U S A 97:8324
Huang X, Margulis CJ, Berne BJ (2003) Dewetting-induced collapse of hydrophobic particles. Proc Natl Acad Sci U S A 100:11953
Kulp JL III, Kulp JL Jr, Pompliano DL, Guarnieri F (2011) Diverse fragment clustering and water exclusion identify protein hot spots. J Am Chem Soc 133:10740
Li J, Liu Q (2009) 'Double water exclusion': a hypothesis refining the O-ring theory for the hot spots at protein interfaces. Bioinformatics 25:743
Malaspina DC, Rodriguez Fris JA, Appignanesi GA, Sciortino F (2009) Identifying a causal link between structure and dynamics in supercooled water. Europhys Lett 88:16003
Malaspina D, Schulz EP, Alarcón LM, Frechero MA, Appignanesi GA (2010) Structural and dynamical aspects of water in contact with a hydrophobic surface. Eur Phys J E 32:35
Nagle JF, Tristram-Nagle S (2000) Structure of lipid bilayers. Biochim Biophys Acta 1469:159
Nickels JD, Katsaras J (2015) Chapter 3: Water and lipid bilayers. In: Disalvo EA (ed) Membrane hydration: the role of water in the structure and function of biological membranes. Springer, Cham, pp 45–67
Pfeiffer H (2015) Chapter 4: Hydration forces between lipid bilayers: a theoretical overview and a look on methods exploring dehydration. In: Disalvo EA (ed) Membrane hydration: the role of water in the structure and function of biological membranes. Springer, Cham, pp 69–104

Qvist J, Davidovic M, Hamelberg D, Halle B (2008) A dry ligand-binding cavity in a solvated protein. Proc Natl Acad Sci U S A 105:6296

Rasaiah JC, Garde S, Hummer G (2008) Water in nonpolar confinement: from nanotubes to proteins and beyond. Annu Rev Phys Chem 59:713

Rehm TH, Schmuck C (2010) Ionpair induced self-assembly in aqueous solvents. Chem Soc Rev 39:3597

Schulz EP, Alarcón LM, Appignanesi GA (2011) Behavior of water in contact with model hydrophobic cavities and tunnels and carbon nanotubes. Eur Phys J E 34:114

Shen YR, Ostroverkhov V (2006) Sum-frequency vibrational spectroscopy on water interfaces: polar orientation of water molecules at interfaces. Chem Rev 106:1140

Shiratani E, Sasai M (1996) Growth and collapse of structural patterns in the hydrogen bond network in liquid water. J Chem Phys 104:7671

Shiratani E, Sasai M (1998) Molecular scale precursor of the liquid–liquid phase transition of water. J Chem Phys 108:3264

Sierra MB, Accordino SR, Rodriguez Fris JA, Morini MA, Appignanesi GA, Fernández SA (2013) Protein packing defects “heat up” interfacial wáter. Eur Phys J E 36:62

Stanley HE, Kumar P, Xu L, Yan Z, Mazza MG, Buldyrev SV, Chen S-H, Mallamace F (2007) The puzzling unsolved mysteries of liquid water: some recent progress. Phys A 386:729

Vitkup D, Ringe D, Petsko GA, Karplus M (2000) Solvent mobility and the protein glass transition. Nat Struct Biol 7:34

Wang L, Berne BJ, Friesner RA (2011) Ligand binding to protein-binding pockets with wet and dry regions. Proc Natl Acad Sci U S A 108:1326

Young T, Abel R, Kim B, Berne BJ, Friesner RA (2007) Motifs for molecular recognition exploiting hydrophobic enclosure in protein–ligand binding. Proc Natl Acad Sci U S A 104:808